

# Optical Detection Development for the Hogan Quantum Holographic Noise Experiment

by

David Bruce Kelley

Submitted to the Department of Physics  
in partial fulfillment of the requirements for the degree of

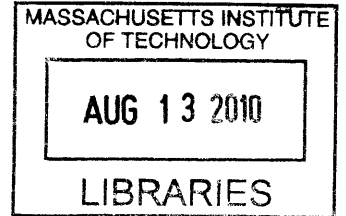
Bachelor of Science in Physics

at the

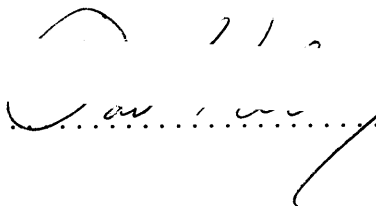
MASSACHUSETTS INSTITUTE OF TECHNOLOGY


June 2010


© Massachusetts Institute of Technology 2010. All rights reserved.

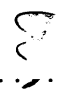


**ARCHIVES**

Author .....  .....  
Department of Physics  
May 18, 2010

Certified by .....  .....  
Nergis Mavalvala  
Professor  
Thesis Supervisor

Certified by .....  .....  
Rainer Weiss  
Professor Emeritus  
Thesis Supervisor

Accepted by .....  ..... *is Supervisor*  
Krishna Rajagopal  
Chairman, Department of Physics



# Optical Detection Development for the Hogan Quantum Holographic Noise Experiment

by

David Bruce Kelley

Submitted to the Department of Physics  
on May 18, 2010, in partial fulfillment of the  
requirements for the degree of  
Bachelor of Science in Physics

## Abstract

Craig Hogan recently proposed a “quantum holographic” noise that could potentially raise the expected noise floor for some current and upcoming high precision interferometers. Rainer Weiss et al. have designed an experiment searching for the noise in two coaligned Michelson interferometers. We have assembled and tested a photodetection system to measure broadband phase correlation between two optical signals, to be used in the noise detection experiment. This included modifying and characterizing photodetectors and setting up a system to record the signal correlation between the two detectors. We altered a LabVIEW program to assist in data collection and explored several ways to improve the data recording rate, which will allow larger data sets and thus longer runs. The detection system had a shot noise limited sensitivity of  $4nV/\sqrt{Hz}$  and allowed for measurements at the level of 1 % correlation.

Thesis Supervisor: Nergis Mavalvala  
Title: Professor

Thesis Supervisor: Rainer Weiss  
Title: Professor Emeritus



## **Acknowledgments**

I'd like to thank Rainer Weiss for inspiration for the project followed by invaluable assistance and strong encouragement along the way. I'd like to thank Stephan Meyer for facilitating my visit to the University of Chicago and helping me understand the instrumentation and the calculations. I'd like to thank Nergis Mavalvala and my parents for editing and advice. I'd also like to acknowledge Emma Tolley for her illustration of Figure 3-2 and editing help.

I'd also like to thank the MIT UROP program for funding my research as an undergraduate student and the University of Chicago Department of Physics for funding my stay in Chicago.



# Contents

<b>1</b>	<b>Introduction</b>	<b>11</b>
1.1	Quantum Holographic Noise . . . . .	11
1.2	Proposed Experiment . . . . .	12
<b>2</b>	<b>The Photodetectors</b>	<b>15</b>
2.1	Overview of the detector and modifications . . . . .	15
2.1.1	Calculation for DC gain . . . . .	15
2.1.2	Calculation for AC gain . . . . .	16
2.2	Calculation for shot noise . . . . .	17
2.2.1	The Diode . . . . .	17
2.3	Characterizing the detectors . . . . .	18
2.3.1	Measuring AC and DC gain . . . . .	18
2.3.2	AC transfer function . . . . .	18
2.3.3	Shot noise measurements . . . . .	19
2.3.4	Discrepancies in shot noise . . . . .	21
<b>3</b>	<b>Correlation Detection</b>	<b>23</b>
3.1	Test of correlation detection . . . . .	23
3.2	Filtering . . . . .	26
3.3	Analysis . . . . .	26
<b>4</b>	<b>Results and Conclusions</b>	<b>29</b>
4.1	Results . . . . .	29

4.2 Conclusions . . . . .	29
<b>A LABview Program</b>	<b>33</b>



# List of Figures

1-1	Diagram of the proposed experiment. . . . .	13
2-1	Circuit diagram of the photodetector . . . . .	16
2-2	AC gain of the two sensors . . . . .	18
2-3	AC transfer functions . . . . .	19
2-4	Shot noise response of the modified PDA 255s . . . . .	20
3-1	Theoretical prediction . . . . .	25
3-2	Correlation test setup . . . . .	25
3-3	Shot noise experienced by a detector . . . . .	28
4-1	Parallel sensor correlation spectrum. Used with permission from Stephan Meyer. . . . .	30
4-2	Split sensor correlation spectrum. Used with permission from Stephan Meyer. . . . .	31
A-1	Screen shot of the LABView program . . . . .	34



# Chapter 1

## Introduction

High-precision laser interferometry is used in currently operating observatories that are searching for gravitational waves from the universe. Interferometric gravitational wave detectors are being built today to higher precision than ever before. Every possible noise source is carefully studied and minimized. A new noise source would thus be of great interest to physicists studying gravitational waves, especially if it was significant enough to affect the operation of their detectors.

### 1.1 Quantum Holographic Noise

In several recent papers[2][3][4], Craig Hogan described a new, unexpected background noise source dubbed “quantum holographic” noise. Hogan describes this as “a surprisingly large quantum indeterminacy in the relative transverse positions of events. These appear in the 3D world as apparent fluctuations in the metric with a distinctive, purely transverse spatial shear character ... and a flat, frequency-independent spectrum.”[4]. In other words, this proposed noise is due to quantum fluctuations on the exterior limit of the observable universe, projected holographically inwards on the 3D visible universe.

Hogan posits that the quantum holographic fluctuations will cause a jitter transverse to the direction of propagation in the laser beam,  $\delta\theta = \left(\frac{l_{Pl}}{L}\right)^{1/2}$  a function of  $l_{Pl} = \sqrt{\frac{\hbar G}{c^3}}$ , the Planck Length, and L, the interferometer arm length. When the light hits

a beamsplitter (at 45 degrees), this will convert into a change in the distance traveled by the light,  $\delta x = L\delta\theta = (l_{Pl}L)^{1/2}$  as the beam hits different parts of the splitter. This will in turn cause a phase noise  $\delta\phi = 2\pi\frac{\delta x}{\lambda_{laser}} = \frac{2\pi}{\lambda_{laser}}(l_{Pl}L)^{1/2}$

If another interferometer is similarly aligned and occupies some of the same space, the noise due to this effect should be correlated between the two interferometers. This is because  $\delta\theta$  is a property of the space time that the interferometer beam is passing through; if one piece of space time jitters, nearby points should as well. If we can measure this correlation, it will give strong support to Hogan's theory.

## 1.2 Proposed Experiment

We seek to measure the correlations in the optical phase fluctuations at the antisymmetric ports of two 40 meter Michelson interferometers placed next to each other (see Figure 1-1 [9]). The goal of this experiment is to detect a small correlation over a large frequency range between two photodetectors. For filtering, our low frequency bound will be set by seismic and environmental noise at about 50 KHz. The upper bound should be at least the travel time of light over arm length,  $\frac{c}{2L} \approx 3.75\text{MHz}$ . It will be set at 5 MHz.

In the operation of the experiment, one or both of the end stations of one of the interferometers will be portable. This will allow variation of the separation between the interferometers, and thus vary the correlation coefficient.

There were two main phases of this project. During the first phase, we worked with individual PDA 255 photodetectors to improve and characterize their frequency response and noise. The second phase was the development and testing of correlation detection between a pair of PDA 255s in a setup that simulated the conditions in the proposed experiment.

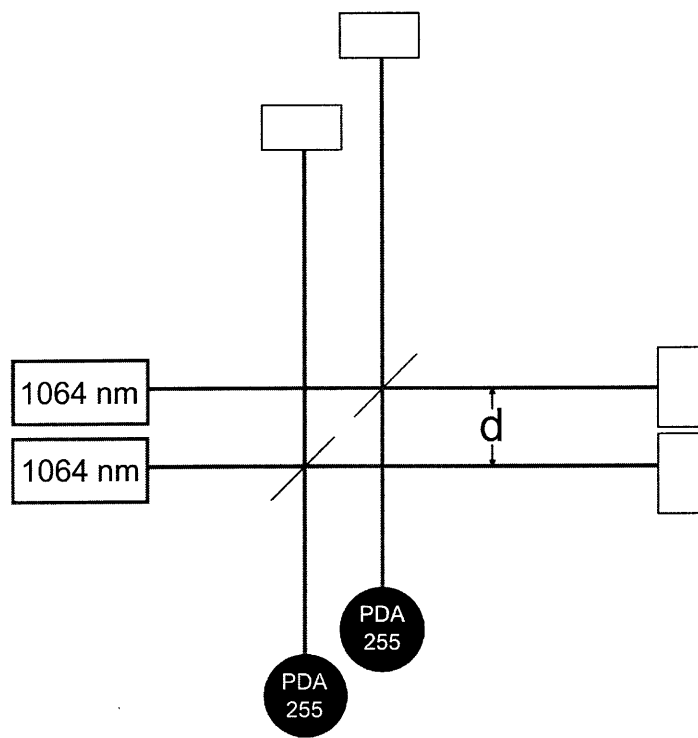


Figure 1-1: Diagram of the proposed experiment. It uses two isolated 1064 nm Michelson interferometers located close together. Changing the distance  $d$  between the interferometers should cause the degree of noise correlation measured at the photodetectors to change.



# Chapter 2

## The Photodetectors

To measure shot noise, we had to modify the detectors raise the AC gain while keeping the DC gain low. This allowed us to measure the detector shot noise without being swamped by the DC photo current. We did this by adding two more capacitors to the circuit, C1 and C2 in Figure 2-1. This way, we could measure the shot noise in the AC output and compare it to the expected value calculated from the DC output.

### 2.1 Overview of the detector and modifications

The photodetectors used were originally Thorlabs PDA255, InGaS detectors with a 700-1800nm sensitivity and a signal response of about 50MHz. The diagram in Figure 2-1 shows the modified circuit diagram of the device. With these modifications, we can measure the shot noise in the AC signal without it saturation by the photo current.

#### 2.1.1 Calculation for DC gain

The DC gain of the circuitry is a straightforward. With unity gain in the two amplifier stages due to the two inserted capacitors, the only significant contribution is the  $50\Omega$  resistance of R9, which will have the effect of a voltage divider when put in series with a  $50\Omega$  load. The Intersil HA-5002 buffer has a gain of 0.971, so the expected

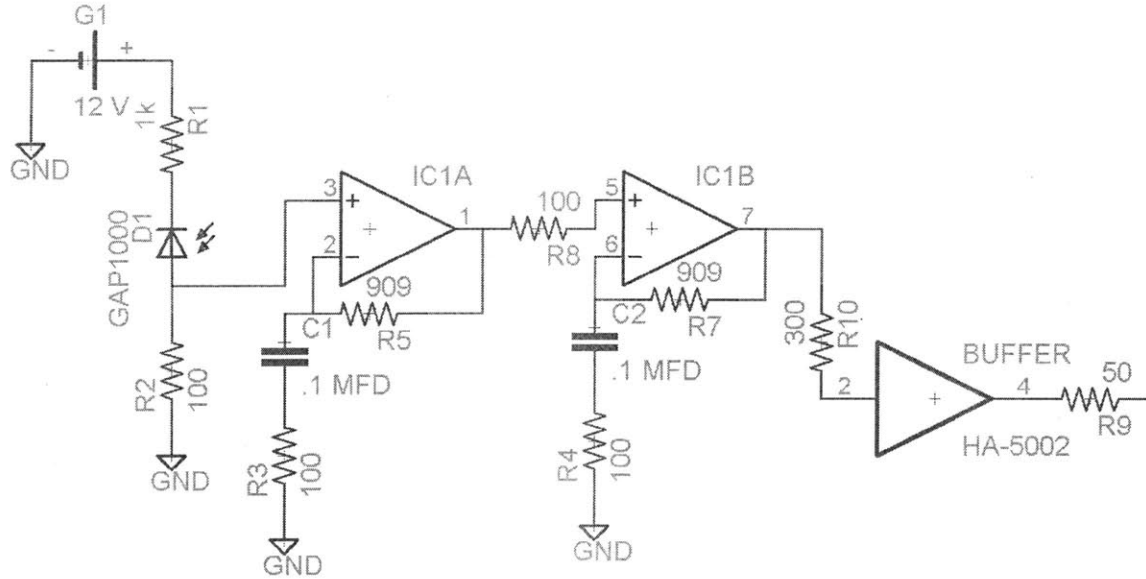


Figure 2-1: Circuit diagram of the modified PDA 255 photodetectors. The capacitors were added to increase the AC gain and decrease the DC gain of the amplification circuits.

DC gain is  $.5 \times .971 = 0.486$ .

### 2.1.2 Calculation for AC gain

The AC gain of the circuits is more complicated. We still have the  $50\Omega$  divider at the end, as well as the 0.971 gain buffer.

$$G = \left(1 + \frac{R5}{R3}\right) \left(1 + \frac{R7}{R4}\right) \left(\frac{50\Omega}{100\Omega}\right) 0.971 = 49.43 \quad (2.1)$$

This is obviously a high frequency limit calculation. We expect to see the gain rise from 0.5 up to 49 as it climbs up in frequency, leveling out before 1 MHz. We would also expect some resonance features and a gentle roll-off due to the finite gain-bandwidth product of the op-amps.



## 2.2 Calculation for shot noise

We can calculate the shot noise  $v(f)$  (in  $nV/\sqrt{Hz}$ ) from the photocurrent flowing through the resistor R2 in Figure 2-1, based on the output DC voltage from the photodetector. The voltage due to the photocurrent is amplified by the DC gain. We used noise voltage with spectral density

$$v(f) = \sqrt{2IR^2} \quad (2.2)$$

as a test of the noise levels in the detector. This noise should also be broadband, so it is a good representation of what we expect to be looking for. We used the expected noise as a measure of the other noise in the system. If we see only the noise expected from the shot noise, we can be fairly certain that the diode itself is the limiting factor in the detector.

Knowing the AC and DC gains of the photodetectors, we can use the DC output of the detectors to predict the current through R2 and thus the shot noise via Equation 2.2. we can also measure the noise directly, as the AC output. The hope is that these values will agree, showing that there are no other significant noise sources affecting the detectors.

### 2.2.1 The Diode

The photodetectors use a large area InGaAs photodiode (the GAP 1000 made by GPD) [1]. They are intended for use in the IR range and have a large (1 mm diameter) active sensing region. This makes them ideal for sensing lower power IR laser light, such as a 1064 nm Nd:YAG laser.

## 2.3 Characterizing the detectors

### 2.3.1 Measuring AC and DC gain

The DC gain of the circuit was measured directly. A power supply was connected to the circuit across the signal resistor R2, and the output voltage measured. The values recorded were roughly as expected: sensor 1 had a gain of 0.477 and sensor 3 had a gain of 0.487.

To measure the AC gain of the detectors, we used the same method as the DC gain. We put a signal across R2 and measured the output voltage levels as functions of frequency. The calibrated output is plotted in Figure 2-2. To calibrate, we calculated low frequency gains were using a lower-frequency analyzer, and the higher frequency points, taken on a different analyzer, were scaled so that at 50 kHz, the two analyzers' values were equal.

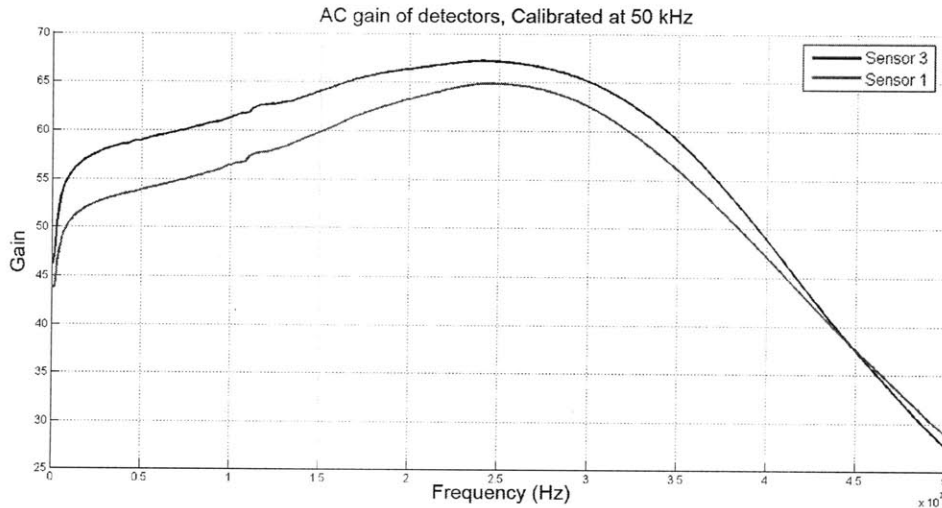


Figure 2-2: AC gain of the two sensors. Data taken using an RF modulated diode laser.

### 2.3.2 AC transfer function

Figure 2-3 shows the measured transfer functions of the two detectors. These measurements were taken using an amplitude modulated IR laser diode that could go up

past 50 MHz. Since the diode and the detector spectra were not perfectly flat, we normalized them using a more accurate New Focus 1811 IR detector. The base value was set by the electronic gain at 50KHz. The most important aspect shown in these diagrams is the smooth behavior of the phase response: This will be essential because the experiment will be measuring phase noise.

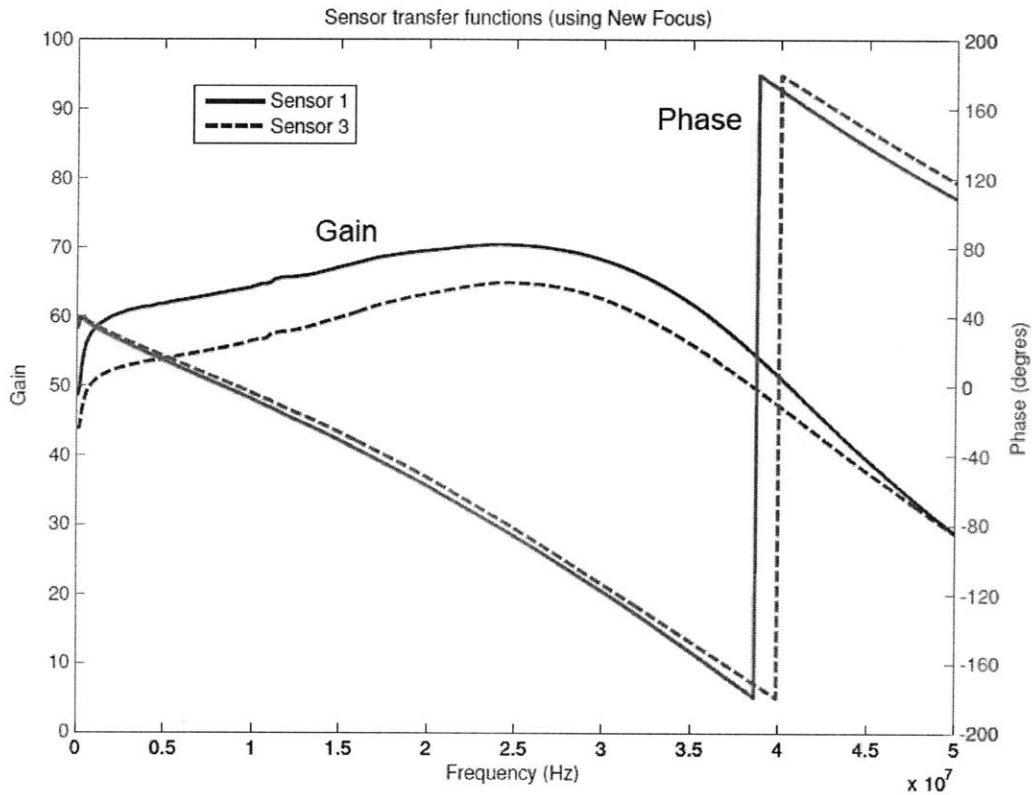


Figure 2-3: Magnitude and phase transfer functions for the two sensors. This is a scaled measurement that incorporates the AC gain with the photodiode response to reflect how the detector will respond to a certain frequency of light.

### 2.3.3 Shot noise measurements

As mentioned previously, we can get a theoretical value for the shot noise in the detector from the DC output and a measured value for the total noise from the AC output. If these are the same, we can comfortably say that the detectors are operating

at the limits of the diode.

To test this, we used a halogen light bulb with a tungsten filament as a black body thermal radiation emitter. The source affords high power in a small package, which allows us to maximize the power received by placing the bulb very close to the detector. The goal of putting this much power onto the detectors was to raise the shot noise to the point where the voltage output was in the normal operating region and the shot noise dominated over the detector noise. Once in the proper operating region, we could compare the shot noise to the other noise sources. We then compared this result with the expected values, shown in Figure 2-4.

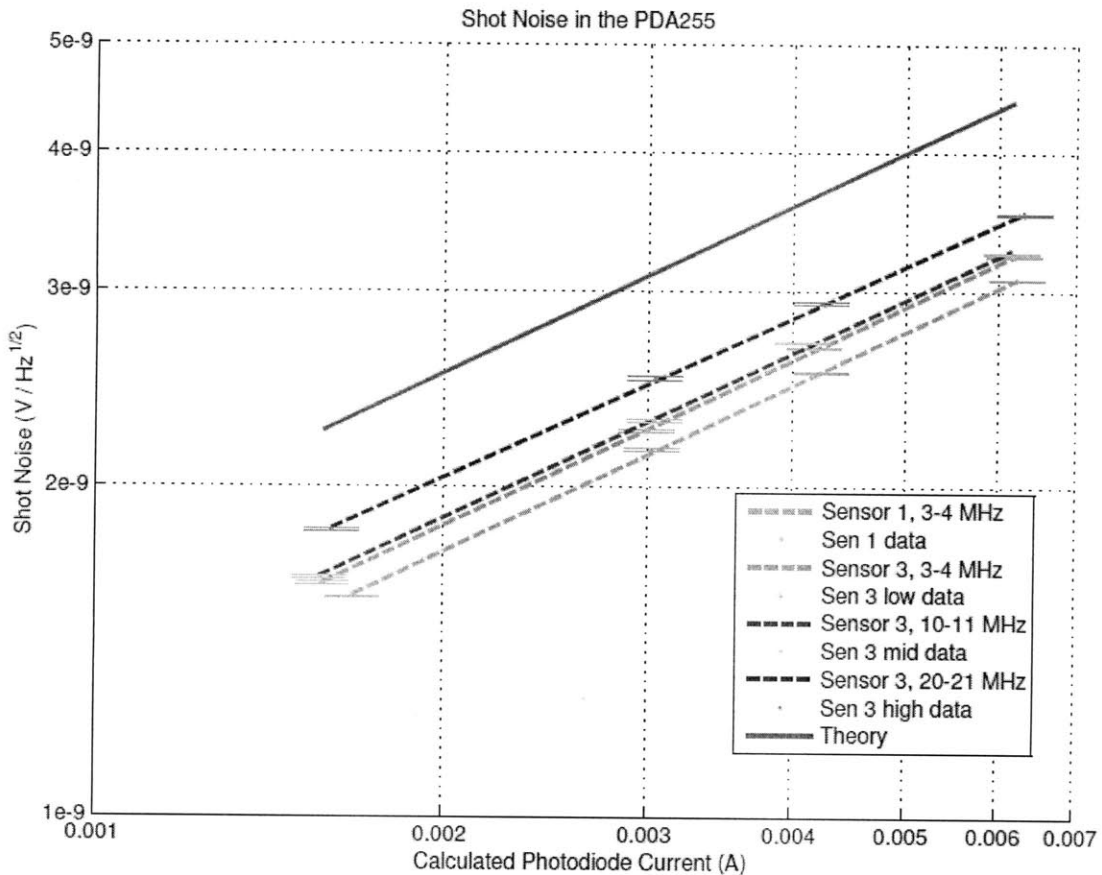


Figure 2-4: Shot noise for two detectors and in a variety of frequency ranges. Points with error bars are the data taken, the dashed lines are fits. The higher frequency shot noise fits are closer to the expected value than the lower ones.

As you can see from Figure 2-4, it appears that the detectors saw lower noise than is to be expected from shot noise.

### **2.3.4 Discrepancies in shot noise**

The shape of the measured curves agree with the theoretical value, but there is a difference factor between them on the order of 15%.

We installed an IR low pass filter that cut everything above  $0.85 \mu\text{m}$ . This helped some (on the order of 2%) but it did not solve the problem completely.

The reason for this discrepancy is not understood. One possibility is the change in the statistics of the current flow due to space charge in the diode material. A similar reduction in the shot noise occurs in electron vacuum tubes.



# Chapter 3

## Correlation Detection

### 3.1 Test of correlation detection

Once we had an understanding of the detector characteristics, we set out to measure a partially correlated optical signal as a simulation of the final experiment. We sought to test the detection of small amounts of phase correlation with the use of a special property of blackbody radiation[7][6]. In the low frequency part of the blackbody spectrum, the light is partially correlated.

Equation 3.1 gives the blackbody power  $dP$  as a function of  $\nu$  the optical frequency and  $T$  the blackbody temperature, for a bandwidth  $d\nu$ . It also includes two other terms based on the physical setup, shown in Figure 3-2:  $A\Omega$  and  $\epsilon(\nu)$ .  $A\Omega$  is the étendue, a measure of how much emitted light actually goes into the detector. We calculate this value, the area  $A$  times the solid angle  $\Omega$  of light at the apertures and choose the smallest value. In our case the limiting factor is the light going from the smaller lenses into the detectors.  $\epsilon(\nu)$  is the total efficiency of the optics, which we calculate to be roughly flat,  $\epsilon_{splitter}\epsilon_{detector}\epsilon_{lens}^2 = 0.50 \cdot 0.80 \cdot 0.94^2 \cdot 0.37 = 0.13$ .

$$dP(\nu, T) = A\Omega\epsilon(\nu)\frac{2h\nu^3}{c^2(e^{h\nu/kT} - 1)}d\nu \quad (3.1)$$

To determine the power incident upon one of our detectors, we can integrate  $dP(\nu, T)$ .

$$P = \int dP(\nu, T) = \int_{f_1}^{f_2} A\Omega\epsilon(\nu) \frac{2h\nu^3}{c^2(e^{h\nu/kT} - 1)} d\nu \quad (3.2)$$

It has been shown that the photons emitted from a black body in the so called “Rayleigh-Jeans” region, where the frequency is lower than the peak frequency, will tend to arrive in groups, because a single random photon emission tends to stimulate more photon emissions. The measure of this stimulated emission is the photon occupation number,

$$\frac{\epsilon(\nu)}{(e^{h\nu/kT} - 1)} \quad (3.3)$$

The photon occupation number determines how the photon noise equivalent power, given in Equation 3.4 behaves.

$$\langle \Delta P^2 \rangle = \int 2h\nu dP \left( 1 + \frac{\epsilon(\nu)}{(e^{h\nu/kT} - 1)} \right) \quad (3.4)$$

At high frequencies when the photon occupation number is small, the photon noise simplifies to the shot noise equation

$$\langle \Delta P_{shot}^2 \rangle = \lim_{h\nu/kT \rightarrow \infty} \int 2h\nu dP \quad (3.5)$$

When the frequency is low and the occupation number is large Equation 3.4 becomes

$$\langle \Delta P_{corr}^2 \rangle = \lim_{h\nu/kT \rightarrow 0} \int 2h\nu dP \frac{\epsilon(\nu)}{e^{h\nu/kT} - 1} = \frac{4k^2T^2 A\Omega}{c^2} \int_{f_1}^{f_2} \epsilon(\nu) \nu^2 d\nu \quad (3.6)$$

For the source, we used a projector lamp with a filament temperature  $T$  of about 2500 kelvin, which we assumed to be roughly equivalent to a thermal emitting black-body. Through the addition of a  $0.85\mu\text{m}$  low pass optical filter to the front of each detector, we limit the high frequency, noncorrelated light, coming into the detector. The frequency is bounded at about  $1.7\mu\text{m}$  on the lower end by the detector response.

We integrate Equation 3.2 from  $c/0.85$  to  $c/1.7\mu\text{m}$  to get a total power of 16.7 mW incident on the detector and integrate Equation 3.4 over the same bounds to get



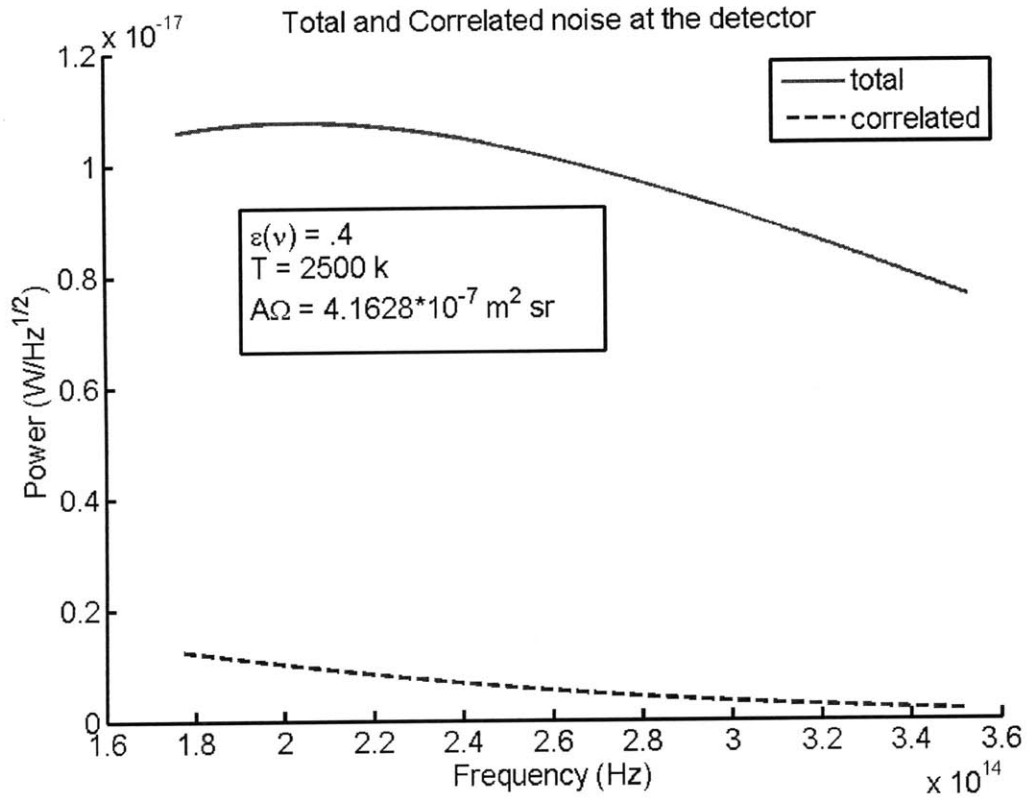


Figure 3-1: Theoretical predictions for  $\Delta P_{total}(\nu)$  and  $\Delta P_{corr}(\nu)$  based on Equation 3.4

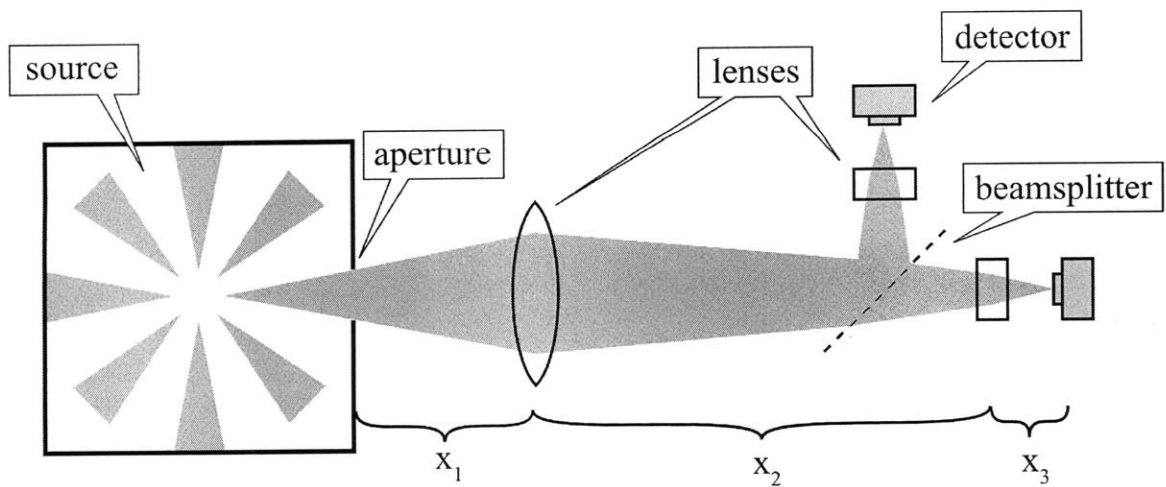


Figure 3-2: Diagram of the correlation setup used to evaluate the photodetectors.  $x_1 = 82.1 \text{ mm}$ ,  $x_2 = 869 \text{ mm}$ ,  $x_3 = 20.5 \text{ mm}$ .

a total noise power of  $7.4 \times 10^{-11}W/\sqrt{Hz}$ . If we integrate only the correlated part of the noise in Equation 3.4, we get  $2.8 \times 10^{-12}W/\sqrt{Hz}$ , or about 4% of the total noise.

## 3.2 Filtering

There were several filters applied to the input signal at different times.

The first filter is an optical filter placed in front of the detector. This is a low-pass IR filter, passing wavelengths longer than  $0.85\mu\text{m}$ . The detector itself only responds to wavelengths up to about  $1.7\mu\text{m}$  [8], so this defines our optical bandwidth.

There is a capacitor on the line in to the digitizer, which combines with the  $50\Omega$  impedance of the amplifier to create a high pass filter with a fairly low cutoff, effectively blocking DC signals from overloading the digitizer, without changing the interesting part of the signal.

The digitizer also has a built in 20 MHz Bessel filter, to keep the signal below the Nyquist frequency of 25 MHz (we sampled at 50 MHz).

## 3.3 Analysis

We took three types of data for comparison: dark, with no light falling on the active detectors; parallel, with the two active detectors pointing directly at the source (without a beam splitter, so the two detectors see different parts of the filament, precluding correlated photon reception); and split, with the setup exactly as it appears in 3-2 (this way we can put the image of the same part of the filament on both detectors). The correlation between the two the split detectors minus the correlation between the two parallel detectors should show our total correlated noise.

The digitizer we used (see Appendix A) wrote the two channels to the data file in chunks of 2097152, so this was the easiest set size to analyze. For basic analysis we calculate a power spectrum for the inputs. This is demonstrated in Equation 3.7, where  $F(x)$  is the Fourier transform of  $x$ , the data for a given channel, and  $n$  is the number of data points, in this case 2097152. This allowed us to identify noise sources

and maximize the light entering both detectors.

$$P(\nu, x) = \frac{|F(x)|^2}{n/2} \quad (3.7)$$

Next, we look for the cross-correlation between the two detectors. The cross-correlation is a measure of the similarity of two signals as a function of time lag in one relative to the other. For a given time lag  $t$ ,

$$m \star n = \int_{-\tau_0}^{\tau_0} m^*(\tau)n(t + \tau)d\tau \quad (3.8)$$

is the correlation between the two functions, and  $C(t)$  is the normalized correlation coefficient, ranging from -1 to 1.

$$C(t) = \frac{m \star n}{Norm} = \frac{\int_{-\tau_0}^{\tau_0} m^*(\tau)n(t + \tau)d\tau}{\sqrt{\int_{-\tau_0}^{\tau_0} m^2(\tau)d\tau \int_{-\tau_0}^{\tau_0} n^2(\tau)d\tau}} \quad (3.9)$$

Where  $\tau_0$  is the integration time, which should be longer than any feature we want to resolve. We can also bring this to the frequency domain, by taking the Fourier transforms  $F$  of the input signals. In this case, we can determine the Fourier transform of the correlation  $m \star n$ .

$$F(m \star n) = F(m) \cdot F(n)^* \quad (3.10)$$

This is a useful tool because we can compute the cross spectrum without going through the trouble of using Equation 3.9.

We can also consider the percent correlation in the Fourier domain.

$$C_p = \frac{\sum \Re[F(m(\nu))^*F(n(\nu))]}{\sqrt{(\sum |m(\nu)|^2) (\sum |n(\nu)|^2)}} \quad (3.11)$$

This is a calculation of the fraction of correlated to uncorrelated signals for  $m$  and  $n$ . By subtracting the

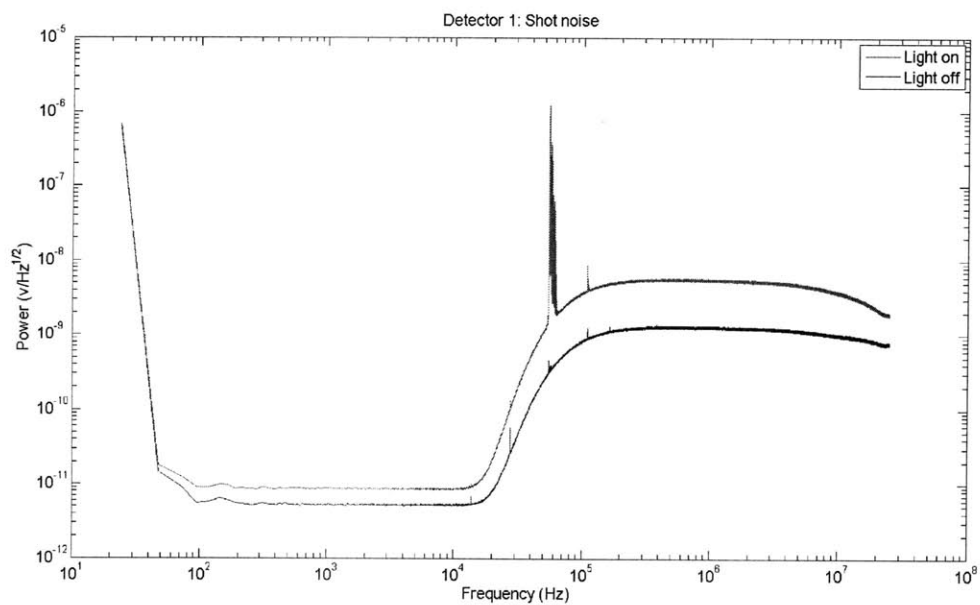


Figure 3-3: Comparison of power seen by an illuminated (split) detector and a dark detector. This difference is due to the photon shot noise. The differences between split and parallel are small on this scale, so only one is shown for reference.

# Chapter 4

## Results and Conclusions

### 4.1 Results

We ran into an error in normalization for the cross spectrum, so we have included plots created by Stephan Meyer. These plots show the correlation spectrum between the two sensors for the parallel (Figure 4-1) and split (Figure 4-2) detectors.

Using Equation 3.11 over the frequency range of 150 kHz to 5MHz, we arrived at a normalized correlation fraction difference of  $(7 \pm 7) \times 10^{-3}$  between the split and parallel data, which is not statistically significant. It appears we will need longer data sets to make an accurate measurement

### 4.2 Conclusions

We successfully modified two PDA photodetectors and characterized them in the LIGO lab at MIT. The data collected was used in the proposal[5] for funding of the double interferometer experiment, known as the Fermilab Holometer, to be built at Fermilab. The photodetectors were transported and installed at the Meyer Physics Lab in the University of Chicago. The correlation detection system was set up and tested, but it appears that it requires more testing.

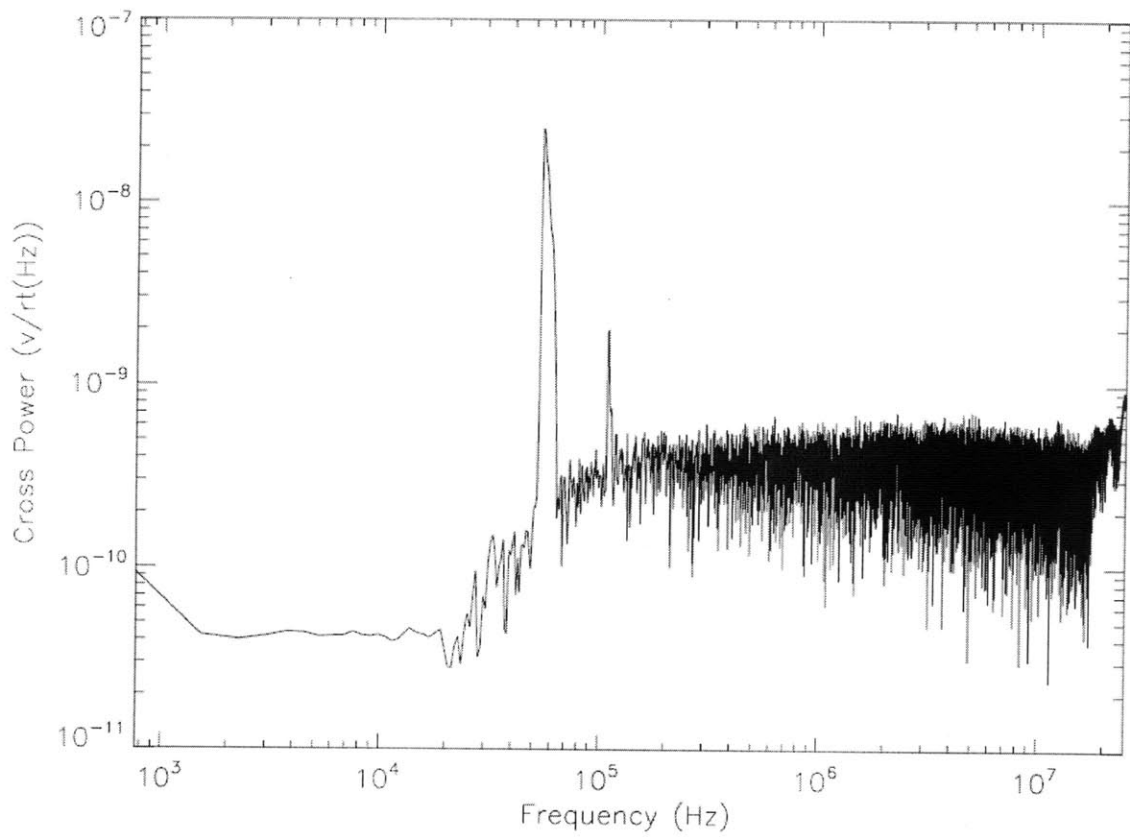


Figure 4-1: Parallel sensor correlation spectrum. Used with permission from Stephan Meyer.

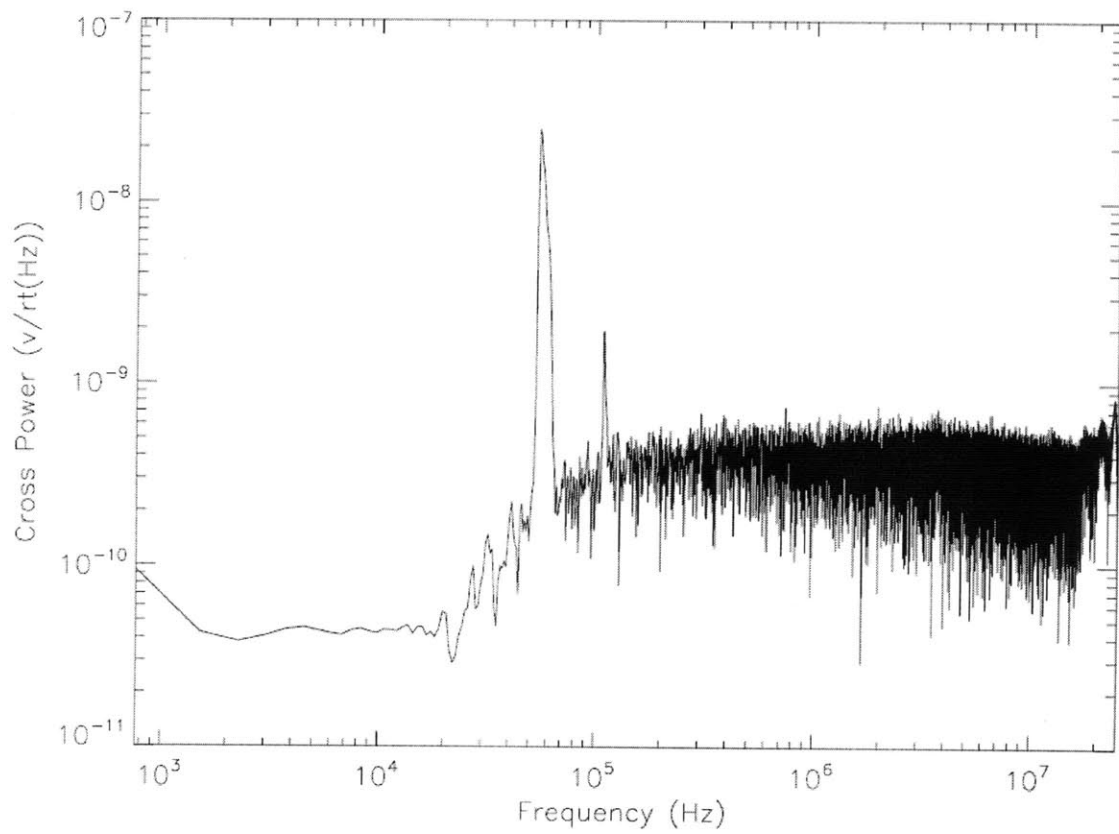


Figure 4-2: Split sensor correlation spectrum. Used with permission from Stephan Meyer.





# Appendix A

## LABview Program

To read the signal from the photodetectors, we use a National Instruments two channel digitizer (PXIe-5122). It can simultaneously sample two channels at 50 megasamples(MS) per second, at 14 bit accuracy. We have two of these devices in a NI PXIe-1075 case, writing to a 12-disk 3 terabyte RAID-0 array (HDD-8264).

Using LABview on Windows XP, we were able to read the data from both channels (16 bit integers at 50 MS/sec = 100 MB/sec) and write it to the drive array. This required bypassing the write buffer that Windows normally uses, going as close to the hard drive driver as possible.

There were some difficulties dealing with 200 MS/sec, as would be experienced if you were running two digitizers simultaneously. It appeared to be Windows related.

I modified the existing program to give it real time output sampling, performing power spectra and cross-correlation on the incoming signals on the fly. This required dropping a significant number of data points periodically such that the digitizer buffers would not overflow, but it allowed us to look at a sample of the output before we began taking data, saving valuable time in the development stages.

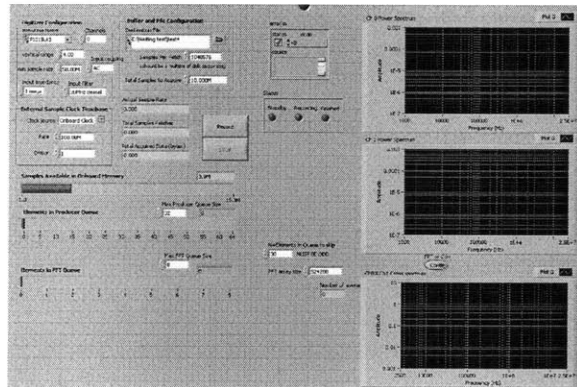


Figure A-1: Screen shot of the LABView program with displays for the preview output.

# Bibliography

- [1] GPD Optoelectronics Corp., <http://gpd-ir.com/pdf/LARGEAR.pdf>. *Large Area InGaAs Photodiodes*, April 2003.
- [2] Craig J. Hogan. Holographic discreteness of inflationary perturbations. *Phys. Rev. D*, 66(2):023521, July 2002.
- [3] Craig J. Hogan. Indeterminacy of holographic quantum geometry. *Phys. Rev. D*, 78(8):087501, October 2008.
- [4] Craig J. Hogan. Measurement of quantum fluctuations in geometry. *Phys. Rev. D*, 77(10):104031, May 2008.
- [5] Craig J. Hogan and others. The fermilab holometer: A program to measure planck scale indeterminacy, November 2009.
- [6] J. M. Lamarre. Photon noise in photometric instruments at far-infrared and submillimeter wavelengths. *Applied Optics*, 25:870, March 1986.
- [7] Stephan S. Meyer. Correlation measurement test. unpublished technical note, November 2009.
- [8] Thorlabs inc., <http://www.thorlabs.com/Thorcat/2200/2241-D02.pdf>. *Operating Manual PDA255 - High Speed Amplified InGaAs Detector*, August 2000.
- [9] Rainer Weiss. “concept for an interferometric test of hogan’s quantum geometry hypothesis”. 2009.